Interstrand Side Chain−Side Chain Interactions in a Designed β-Hairpin: Significance of Both Lateral and Diagonal Pairings

Faisal A. Syud, Heather E. Stanger, and Samuel H. Gellman*

Contribution from the Department of Chemistry, University of Wisconsin, Madison, Wisconsin 53706

Received April 16, 2001

Abstract: The contributions of interstrand side chain−side chain contacts to β-sheet stability have been examined with an autonomously folding β-hairpin model system. RYVEV^{D}PGOKILQ-NH$_2$ (^{D}P = D-proline, O = ornithine) has previously been shown to adopt a β-hairpin conformation in aqueous solution, with a two-residue loop at D-Pro-Gly. In the present study, side chains that display interstrand NOEs (Tyr-2, Lys-9, and Leu-11) are mutated to alanine or serine, and the conformational impact of the mutations is assessed. In the β-hairpin conformation Tyr-2 and Leu-11 are directly across from one another (non-hydrogen bonded pair). This "lateral" juxtaposition of two hydrophobic side chains appears to contribute to β-hairpin conformational stability, which is consistent with results from other β-sheet model studies and with statistical analyses of interstrand residue contacts in protein crystal structures. Interaction between the side chains of Tyr-2 and Lys-9 also stabilizes the β-hairpin conformation. Tyr-2/Lys-9 is a "diagonal" interstrand juxtaposition because these residues are not directly across from one another in terms of the hydrogen bonding registry between the strands. This diagonal interaction arises from the right-handed twist that is commonly observed among β-sheets. Evidence of diagonal side chain−side chain contacts has been observed in other autonomously folding β-sheet model systems, but we are not aware of other efforts to determine whether a diagonal interaction contributes to β-sheet stability.

Introduction

β-Sheet is a very common substructure in folded proteins. Elucidating the origins of β-sheet stability will contribute to our understanding of protein conformational stability[1] and to our ability to design new peptides with specific structures and/or functions.[2−5] One approach to characterizing intrinsic conformational preferences involves small peptides that fold autonomously to a particular secondary structure in solution. The forces that influence conformational stability can be elucidated by determining how mutations affect the population of the folded state. This strategy has been widely employed for helices[6−8] and β-turns,[9] but application to β-sheet has been limited because well-defined β-sheet model systems have only recently become available.[10,11] As an alternative, secondary structure conformational preferences can be examined within a particular tertiary structure; this approach has been applied to β-sheet structure.[12−15] Implementation of this strategy requires minimization of "context effects", which are not always clearly

defined,[16,17] so that mutations affect conformational stability through secondary structural contacts rather than tertiary structural contacts. In principle, identification of context effects should be simpler in autonomously folding secondary structure models because the molecules themselves are simpler. However, quantitative analysis of mutational effects is more difficult in autonomously folding secondary structure models than in tertiary structure models, because of the marginal stability of the former. Thus, these two approaches are complementary to one another.

Here, we probe the forces that stabilize an autonomously folding β-sheet secondary structure model system previously developed in our laboratory. Our model system is based on the β-hairpin motif, in which two antiparallel strands are connected by a short loop.[18−22] The significance of interstrand side chain−side chain interactions has previously been examined in model systems involving either designed β-hairpins[23−28] or solvent-

* To whom correspondence should be addressed: (e-mail) gellman@chem.wisc.edu.

(1) Nesloney, C. L.; Kelly, J. W. *Bioorg. Med. Chem.* **1995**, *4*, 739−766.

(2) Ghosh, I.; Chmielewski, J. *Chem. Biol.* **1998**, *5*, 439−445.

(3) Nowick, J. S. *Acc. Chem. Res.* **1999**, *32*, 287−296.

(4) Robinson, J. A. *Synlett* **2000**, 429−441.

(5) Struthers, M. D.; Cheng, R. P.; Imperiali, B. *Science* **1996**, *271*, 342−345.

(6) Baldwin, R. L.; Rose, G. D. *Trends Biochem. Sci.* **1999**, *24*, 26−33.

(7) Bolin, K. A.; Millhauser, G. L. *Acc. Chem. Res.* **1999**, *32*, 1027−1033.

(8) Chakrabartty, A.; Baldwin, R. L. *Adv. Protein Chem.* **1995**, *46*, 141−176.

(9) Rose, G. D.; Gierasch, L. M.; Smith, J. A. *Adv. Protein Chem.* **1985**, *37*, 1−109.

(10) Gellman, S. H. *Curr. Opin. Chem. Biol.* **1998**, *2*, 717−724.

(11) Lacroix, E.; Kortemme, T.; Lopez de la Paz, M.; Serrano, L. *Curr. Opin. Struct. Biol.* **1999**, *9*, 487−493.

(12) Koepf, E. K.; Petrassi, H. M.; Ratnaswamy, G.; Huff, M. E.; Sudol, M.; Kelly, J. W. *Biochemistry* **1999**, *38*, 14338−14351.

(13) Mayo, K. H.; Ilyina, E. *Protein Sci.* **1998**, *7*, 358−368.

(14) Merkel, S.; Sturtevant, J. M.; Regan, L. *Struct. Fold. Des.* **1999**, *7*, 1333−1343. Smith, C. K.; Regan, L. *Acc. Chem. Res.* **1997**, *30*, 153−161.

(15) Clark, P. L.; Liu, Z.-P.; Rizo, J.; Gierasch, L. M. *Nat. Struct. Biol.* **1997**, *4*, 883−886.

(16) Minor, D. L.; Kim, P. S. *Nature* **1994**, *371*, 264−267.

(17) Otzen, D. E.; Fersht, A. R. *Biochemistry* **1995**, *34*, 5718−5724.

(18) Sibanda, B. L.; Thornton, J. M. *Nature* **1985**, *316*, 170−174.

(19) Milner-White, E. J.; Poet, R. *Biochem. J.* **1986**, *240*, 289−292.

(20) Sibanda, B. L.; Blundell, T. L.; Thornton, J. M. *J. Mol. Biol.* **1989**, *206*, 759−777.

(21) Sibanda, B. L.; Thornton, J. M. *J. Mol. Biol.* **1993**, *229*, 428−447.

(22) Gunasekaran, K.; Ramakrishnan, C.; Balaram, P. *Protein Eng.* **1997**, *10*, 1131−1141.

(23) Ramírez-Alvarado, M.; Blanco, F. J.; Serrano, L. *Nat. Struct. Biol.* **1996**, *3*, 604−612.

(24) de Alba, E.; Rico, M.; Jiménez, M. A. *Protein Sci.* **1997**, *6*, 2548−2560.

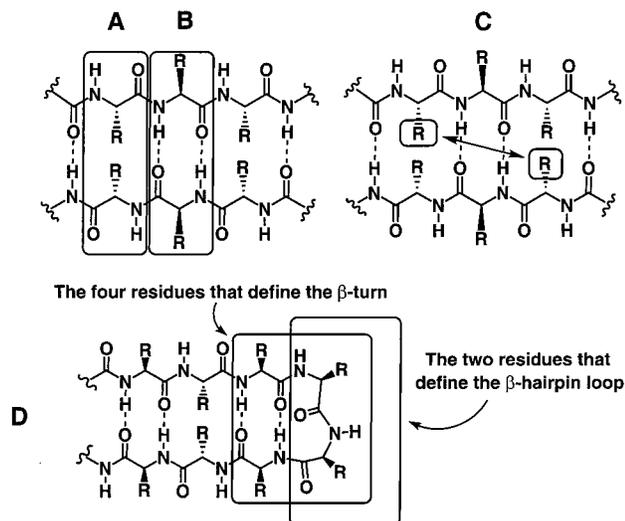(25) Maynard, A. J.; Sharman, G. J.; Searle, M. S. *J. Am. Chem. Soc.* **1998**, *120*, 1996−2007.

Figure 1. Upper: Graphic definitions of (A) non-hydrogen bonded interstrand pairing in antiparallel β-sheet, (B) hydrogen bonded interstrand pairing in antiparallel β-sheet, (C) diagonal interactions in the antiparallel β-sheet. Lower: Relationship between the four residues that define a β-turn and the two residues that define a loop in a tight β-hairpin (a "2:2 β-hairpin", in the nomenclature of Sibanda et al. (ref 20)).

exposed β-sheets in tertiary folding units,[15,17,29,30] and by statistical analysis of protein crystal structures.[31,32] These prior studies, however, have tended to focus on side chains that are directly across from one another in terms of the β-sheet hydrogen bonding registry. We refer to such juxtapositions as "lateral" pairings; the present study considers "diagonal" pairing as well. In antiparallel β-sheet, lateral pairing can involve residues that are not hydrogen bonded to one another ("NHB pairing", Figure 1A) or residues that are hydrogen bonded ("HB pairing", Figure 1B). β-Sheets in proteins usually display a right-handed twist,[33] which should give rise to diagonal contacts (Figure 1C) between side chains that are not directly across from one another in flat projections like Figure 1. Diagonal interstrand contacts have received relatively little attention in the β-sheet literature.

Our approach involves mutational analysis of a designed 12-residue peptide, RYVEV^DPGOKILQ-NH₂ (ref 34), that we have previously shown to display ca. 68% β-hairpin population at 4 °C in aqueous solution.[35] Here, this peptide is designated YKL because residues Tyr-2, Lys-9, and Leu-11 are mutated in the studies described below. YKL contains two nonproteinogenic residues, D-proline (^DP; discussed below) and ornithine (O). Ornithine is structurally related to lysine and arginine. We originally used ornithine so that we could endow the peptide with sufficient positive charge to hinder aggregation while

maintaining the residue diversity necessary for NMR analysis. We have subsequently shown that replacing Orn-8 with Lys has no effect on conformational stability.[35]

YKL
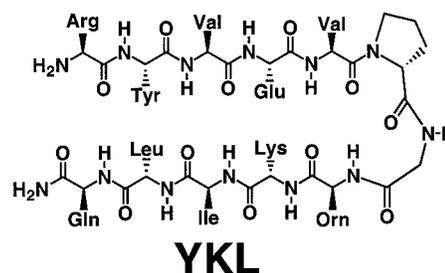
The central D-Pro-Gly segment of YKL forms a two-residue loop in the β-hairpin conformation.[34,36−39] This loop design stems from statistical analysis of β-hairpins in proteins,[19,20] which showed that the most common β-hairpins in folded proteins have two-residue loops, and that these loops generally display type I′ or type II′ β-turn conformations. Type I′ and II′ β-turns are not intrinsically favorable for most L-sequences, but a D-Pro residue at position $i+1$ of a β-turn (i.e., the first of the two loop positions in a two-residue β-hairpin loop (Figure 1D)) strongly favors type I′ and II′ turns.[9] The relationship between β-turn conformation and β-hairpin promotion arises from the right-handed twist preference of β-sheets,[33] which must be matched in the loop. As Sibanda et al. pointed out,[20] the local twist of the common type I and type II β-turns is left-handed, which is not compatible with the strand twist for L-residues. Indeed, replacing D-Pro with L-Pro, which enforces type I and II β-turns,[9] causes total abolition of β-hairpin folding in several designed sequences.[34,36,37,39−41]

The initial NMR analysis of YKL[34] revealed a set of NOEs between the side chains of Tyr-2 and Leu-11, which is consistent with NHB lateral side chain pairing, and another NOE set between the side chains of Tyr-2 and Lys-9, which is consistent with diagonal side chain pairing. These side chain−side chain NOEs led us to suspect that both lateral and diagonal interstrand side chain contacts stabilize the β-hairpin conformation of YKL. NOEs between diagonal side chain pairs have been observed for several other autonomously folding β-sheet model systems;[25,34,40,42−47] however, the fact that these side chains contact one another does not necessarily mean that their proximity contributes to conformational stability. There has been no

(26) Searle, M. S.; Griffiths-Jones, S. R.; Skinner-Smith, H. *J. Am. Chem. Soc.* **1999**, *121*, 11615−11620.

(27) Griffiths-Jones, S. R.; Maynard, A. J.; Searle, M. S. *J. Mol. Biol.* **1999**, *292*, 1051−1069.

(28) Russell, S. J.; Cochran, A. G. *J. Am. Chem. Soc.* **2000**, *122*, 12600−12601.

(29) Blasie, C. A.; Berg, J. M. *Biochemistry* **1997**, *36*, 6218−6222.

(30) Smith, C. K.; Regan, L. *Science* **1995**, *270*, 980−982.

(31) Hutchinson, E. G.; Sessions, R. B.; Thornton, J. M.; Woolfson, D. N. *Protein Sci.* **1998**, *7*, 2287−2300.

(32) Wouters, M. A.; Curmi, P. M. G. *Proteins: Struct. Funct. Genet.* **1995**, *22*, 119−131.

(33) Chothia, C. *J. Mol. Biol.* **1973**, *75*, 295−302.

(34) Stanger, H. E.; Gellman, S. H. *J. Am. Chem. Soc.* **1998**, *120*, 4236−4237.

(35) Syud, F. A.; Espinosa, J. F.; Gellman, S. H. *J. Am. Chem. Soc.* **1999**, *121*, 11577−11578.
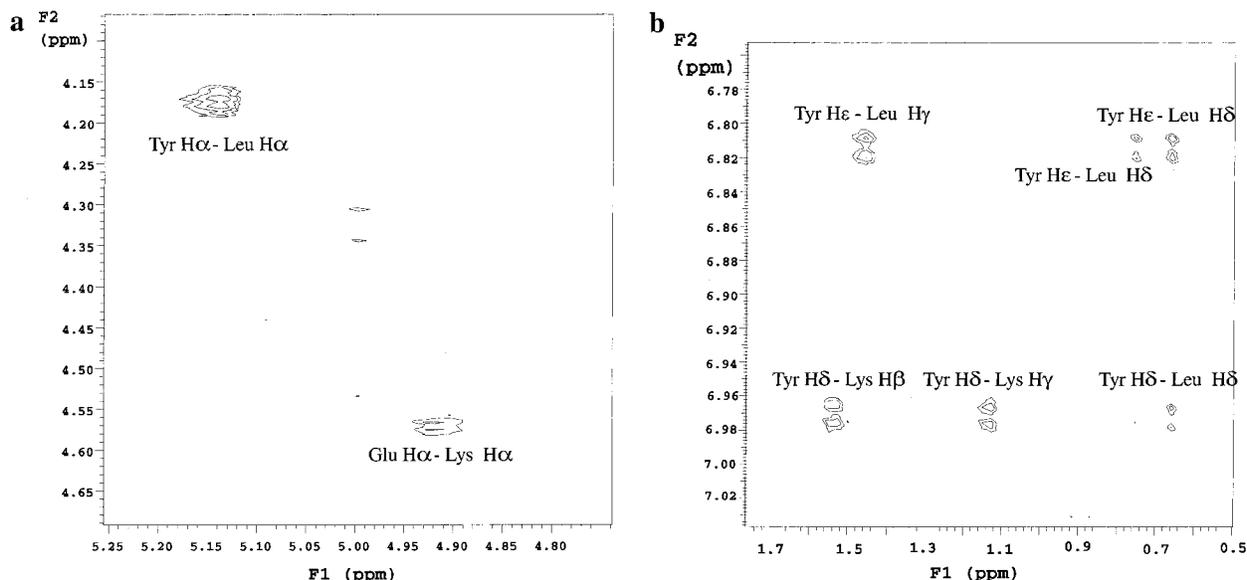
(36) Haque, T. S.; Little, J. C.; Gellman, S. H. *J. Am. Chem. Soc.* **1996**, *118*, 6975−6985.

(37) Haque, T. S.; Gellman, S. H. *J. Am. Chem. Soc.* **1997**, *119*, 2303−2304.

(38) Karle, I. L.; Awasthi, S. K.; Balaram, P. *Proc. Natl. Acad. Sci. U.S.A.* **1996**, *93*, 8189−8193.

(39) Haque, T. S.; Little, J. C.; Gellman, S. H. *J. Am. Chem. Soc.* **1994**, *116*, 4105−4106.

(40) Espinosa, J. F.; Gellman, S. H. *Angew. Chem., Int. Ed.* **2000**, *39*, 2330−2333.

(41) Ragothama, S. R.; Awasthi, S. K.; Balaram, P. *J. Chem. Soc., Perkin Trans. 2* **1998**, 137−143.

(42) Blanco, F. J.; Rivas, G.; Serrano, L. *Nat. Struct. Biol.* **1994**, *1*, 584−590.

(43) Searle, M. S.; Williams, D. H.; Rackman, L. C. *Nat. Struct. Biol.* **1995**, *2*, 999−1006.

(44) Sharman, G. J.; Searle, M. S. *J. Am. Chem. Soc.* **1998**, *120*, 5291−5300.

(45) Triple-stranded designs: Schenck, H. L.; Gellman, S. H. *J. Am. Chem. Soc.* **1998**, 120, 4869−4870. Kortemme, T.; Ramírez-Alvarado, M.; Serrano, L. *Science* **1998**, *281*, 253−256. de Alba, E.; Santoro, J.; Rico, M.; Jiminez, M. A. *Protein Sci.* **1999**, *8*, 854−865.

(46) Andersen, N. H.; Dyer, R. B.; Fesinmeyer, R. M.; Gai, F.; Liu, Z. H.; Neidigh, J. W.; Tong, H. *J. Am. Chem. Soc.* **1999**, *121*, 9879−9880.

(47) Carulla, N.; Woodward, C.; Barany, G. *Biochemistry* **2000**, *39*, 7927−7937.

Figure 2. Selected ROESY data for 2 mM YKL, showing cross-peaks corresponding to key long-range contacts. Data obtained at 4 °C in H_2O/D_2O (9:1 v/v) or in D_2O, 100 mM sodium deuterioacetate buffer, pH 3.8 (uncorrected), 200 ms mixing time, with a Bruker 750 MHz spectrometer. (A) H_α−H_α NOEs. (B) NOEs between the Tyr-2 side chain and the side chains of Lys-9 and Leu-11.

discussion of diagonal side chain−side chain interactions and the possibility that they contribute to β-sheet stability in these previous studies.

In the studies described here we examine the contributions of interstrand side chain−side chain interactions to the stability of the β-hairpin conformation of YKL. These experiments include tests of our hypothesis that the diagonal side chain−side chain contact between Tyr-2 and Lys-9 represents an energetically favorable interaction. To our knowledge, the distinction between lateral and diagonal interactions has not been addressed in previous β-sheet model studies.[14,31,32] Statistical analyses of β-sheet side chain pairing in crystalline proteins have tended to focus on lateral interactions, although one recent study unexpectedly turned up evidence that diagonal interactions could be significant.[48]

Results

Detection and Assessment of β-Hairpin Folding. Observation of NOEs between nonadjacent residues usually provides the most detailed structural insight on compact conformations adopted by peptides in solution.[49,50] YKL displays numerous long-range NOEs; our original examination of YKL at 500 MHz[34] has been extended via ROESY data obtained at 750 MHz. Figure 2 shows selected ROESY data for YKL. NMR data were used for NOE-restrained dynamics with the program DYANA;[51] Figure 3 shows an overlay of the 10 best structures from this analysis (RMSD among these structures is 1.02 ± 0.34 Å (backbone atoms only)). The sideview in Figure 3B highlights the right-handed twist associated with this β-hairpin. We do not observe any NOE for YKL that is inconsistent with the family of β-hairpin conformations shown. Therefore, we conclude that no alternative (nonhairpin) folded conformation is significantly populated for YKL, i.e., that YKL can be treated as a two-state system, unfolded ↔ β-hairpin. The conclusion

(48) Cootes, A. P.; Curmi, P. M. G.; Cunningham, R.; Donnelly, C.; Torda, A. E. *Proteins: Struct. Funct. Genet.* **1998**, *32*, 175−189.

(49) Dyson, H. J.; Wright, P. E. *Annu. Rev. Biophys. Biophys. Chem.* **1991**, *20*, 519−538.

(50) Wüthrich, K. *NMR of Proteins and Nucleic Acids*; Wiley: New York, 1986.

(51) Guntert, P.; Mumenthaler, C.; Wüthrich, K. *J. Mol. Biol.* **1997**, *273*, 283−298.
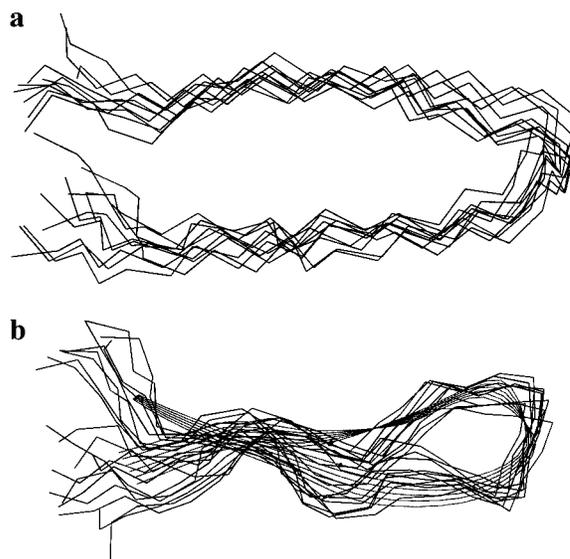

Figure 3. NOE-restrained dynamics results for YKL, using NOEs between protons on nonadjacent residues and NOEs between adjacent residues in the turn region. A total of 500 random structures were annealed by using the program DYANA with NOE restraints derived from NOESY and ROESY data. The RMSD among the best 10 structures was found to be 1.02 ± 0.34 Å. (A) Top view of the 10 best structures of YKL, backbone atoms only. (B) Side-view overlay of the 10 best structures of YKL illustrating the right-handed twist of the hairpin.

that YKL displays a relatively high β-hairpin population in aqueous solution is supported by α-proton chemical shift data,[34] amide proton chemical shift data,[52] and α-carbon-13 chemical shift data.[52]

To study sequence-stability relationships, one requires a method to compare the extent of β-hairpin formation among related peptides. We focus initially on qualitative comparisons among YKL and analogues, including the number and identity of NOEs between nonadjacent residues[50] and the chemical shifts of α-protons ($\delta_{H\alpha}$). Wishart et al.[53] have shown that the

(52) Stanger, H. E.; Syud, F. A.; Espinosa, J. F.; Giriat, I.; Muir, T.; Gellman, S. H. *Proc. Natl. Acad. Sci. USA*, in press.

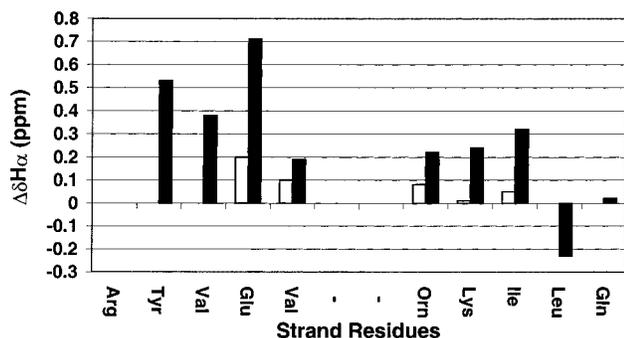**Figure 4.** $\Delta\delta$Hα (observed δHα − random coil δHα) for octamer VEV^{D}PGOKI−NH$_2$ (open bars) and YKL (solid bars). δHα values from YKL-u and octamer-u were used as random coil references. Solvent and NMR conditions are as described in Figure 2.

"chemical shift index" [$\Delta\delta_{H\alpha} = \delta_{H\alpha}$(observed) − $\delta_{H\alpha}$(random coil)] provides qualitative insight on secondary structure. A quantitative approach to β-hairpin population analysis based on $\delta_{H\alpha}$ data is discussed subsequently.

Truncation Suggests That Interstrand Side Chain−Side Chain Interactions Stabilize the β-Hairpin Conformation of Peptide YKL. To determine whether the D-Pro-Gly turn segment is the principal source of β-hairpin stability in YKL, we examined octamer VEV^{D}PGOKI−NH$_2$, the analogue of YKL lacking residues Arg-1, Tyr-2, Leu-11, and Gln-12. Although dodecamer YKL displays numerous NOEs between the side chains of Tyr-2 and Lys-9 or Leu-11, it is impossible to determine from this observation whether interactions among these side chains stabilize the β-hairpin or whether these side chains are brought together by other forces that promote β-hairpin formation. Octamer VEV^{D}PGOKI−NH$_2$ displays no NOEs between nonadjacent residues in aqueous solution at 4 °C. Particularly significant are the absence of the NH- -NH NOE between Val-3 and Orn-6, and the absence of the CαH- -CαH NOE between Glu-2 and Lys-7; the analogous NOEs are observed for YKL. The lack of interstrand NOEs in VEV^D-PGOKI−NH$_2$ suggests that this octamer experiences little or no β-hairpin formation. This conclusion, in turn, suggests that interstrand interactions play a critical role in stabilizing the β-hairpin conformation observed for YKL. (The interstrand interactions might include side chain−side chain interactions involving Tyr-2 and Leu-11 and/or backbone−backbone hydrogen bonds.)

α-Proton chemical shift data [$\Delta\delta_{H\alpha} = \delta_{H\alpha}$(observed) − $\delta_{H\alpha}$(random coil)] for VEV^{D}PGOKI−NH$_2$ support the conclusion that this octamer does not display significant β-hairpin folding in aqueous solution. Figure 4 shows $\Delta\delta_{H\alpha}$ data for VEV^{D}PGOKI−NH$_2$ juxtaposed with $\Delta\delta_{H\alpha}$ data for the analogous residues of YKL. In general, a residue in a β-sheet will display a downfield shifted $\delta_{H\alpha}$ relative to the same residue in an unfolded segment; $\Delta\delta_{H\alpha} \geq +0.1$ is considered significant.[53] Figure 4 shows that the inner strand residues of YKL all display $\Delta\delta_{H\alpha} > +0.1$, which is consistent with a high population of the β-hairpin conformation. In contrast, most of the analogous residues of VEV^{D}PGOKI−NH$_2$ display $\Delta\delta_{H\alpha}$ values near zero, which suggests that this octamer is predominantly unfolded.

The $\delta_{H\alpha}$(random coil) values used to calculate the $\Delta\delta_{H\alpha}$ data for VEV^{D}PGOKI−NH$_2$ and YKL in Figure 4 were obtained from the diastereomeric peptides (VEV^{L}PGOKI−NH$_2$ or RYVEV^{L}PGOKILQ−NH$_2$) in which D-proline is replaced with

L-proline. Extensive previous studies have shown that changing proline configuration completely abolishes β-hairpin formation in designed peptides;[34,36,37,39−41] this point was demonstrated specifically for the L-proline diastereomer of YKL via the absence of any NOEs between nonadjacent residues and other data.[34] Here we designate this L-proline diastereomer YKL-u because it serves as a spectroscopic reference for the *u*nfolded state. $\Delta\delta_{H\alpha}$ values are usually calculated with $\delta_{H\alpha}$(random coil) values obtained either from very short model peptides that cannot fold in water[54] or from averaged $\delta_{H\alpha}$ values derived from protein structure databases.[53] We use L-proline diastereomers to generate $\delta_{H\alpha}$(random coil) values because these reference values should reflect the influence of each strand residue's sequence context.

Mutation at Tyr-2 or Leu-11 Suggests That Both Lateral and Diagonal Interstrand Side Chain−Side Chain Contacts Contribute to β-Hairpin Stability. Two single-site mutants of YKL were examined to determine whether interactions involving the side chains of Tyr-2 and Leu-11 stabilize the β-hairpin conformation. In mutant AKL Tyr-2 is replaced by Ala, and in YKA Leu-11 is replaced by Ala. Qualitative comparisons involving long-range NOEs and $\Delta\delta_{H\alpha}$ data (vide infra) show that both of these mutations lead to a decrease in β-hairpin folding relative to parent peptide YKL. These β-hairpin destabilizations suggest that lateral interaction between the Tyr-2 and Leu-11 side chains contributes to YKL conformational stability. The data indicate also that Tyr-2 → Ala is more destablizing than Leu-11 → Ala, which suggests that the diagonal interaction between Tyr-2 and Lys-9 stabilizes the β-hairpin conformation of YKA.

AKL displays only one NOE involving nonadjacent residues, between NH of Val-5 and NH of Orn-8. This NOE suggests partial population of the loop region of the β-hairpin, but the lack of other interstrand NOEs implies that the β-hairpin conformation is considerably less favorable for AKL than for parent peptide YKL. In contrast, mutant YKA displays multiple NOEs between nonadjacent residues, all of which are consistent with significant population of the expected β-hairpin conformation (Figure 5). Both of the expected CαH- -CαH NOEs are observed for YKA, between Glu-4 and Lys-9 and between Tyr-2 and Ala-11. A strong NOE between CδH of Tyr-2 and CβH$_3$ of Ala-11 and a weaker NOE between CϵH of Tyr-2 and CβH$_3$ of Ala-11 further show that these two residues have adopted the correct lateral orientation in the folded conformation. A set of weak NOEs between CϵH or CδH of Tyr-2 and CβH$_2$, CγH$_2$, or CδH$_2$ of Lys-9 is consistent with contact between these two diagonally juxtaposed side chains. Representative NOE data for YKA are shown in Figure 6. Although the set of nonadjacent NOEs for YKA is consistent with a β-hairpin conformation analogous to that adopted by YKL, differences in NOE intensity and identity suggest that the β-hairpin population of YKA is lower than the β-hairpin population of YKL.

Analysis of $\Delta\delta_{H\alpha}$ data for AKL and YKA (Figure 7) supports our NOE-based conclusions that both mutations decrease β-hairpin stability, and that Tyr-2 → Ala is more deleterious to β-hairpin stability than is Leu-11 → Ala. Parent peptide YKL displays $\Delta\delta_{H\alpha} > +0.1$ at most nonterminal strand residues (Tyr-2 to Val-5 and Orn-8 to Ile-10; Figure 4), and both mutants have smaller $\Delta\delta_{H\alpha}$ values at each of these seven residues. The $\Delta\delta_{H\alpha}$ values for YKA, however, are consistently more positive

(53) (a) Wishart, D. S.; Sykes, B. D.; Richards, F. M. *J. Mol. Biol.* **1991**, *222*, 311−333. (b) Wishart, D. S.; Sykes, B. D.; Richards, F. M. *Biochemistry* **1992**, *31*, 1647−1651.

(54) (a) Schwarzinger, S.; Kroon, G. J. A.; Foss, T. R.; Chung, J.; Wright, P. E.; Dyson, H. J. *J. Am. Chem. Soc.* **2001**, *123*, 2970−2978. (b) Wishart, D. S.; Bigam, C. G.; Holm, A.; Hodges, R. S.; Sykes, B. D. *J. Biomol. NMR* **1995**, *5*, 67−81.
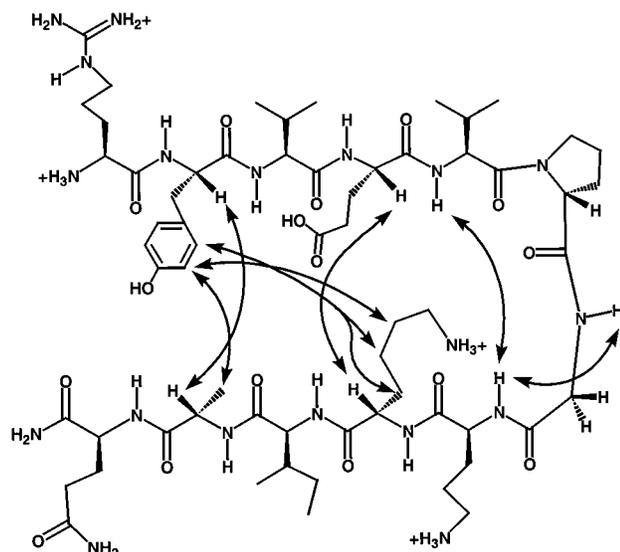
Figure 5. Graphical summary of NOEs between nonadjacent residues observed in ROESY analysis for 2 mM YKA in H_2O/D_2O (9:1 v/v) or in D_2O (conditions described in Figure 2).
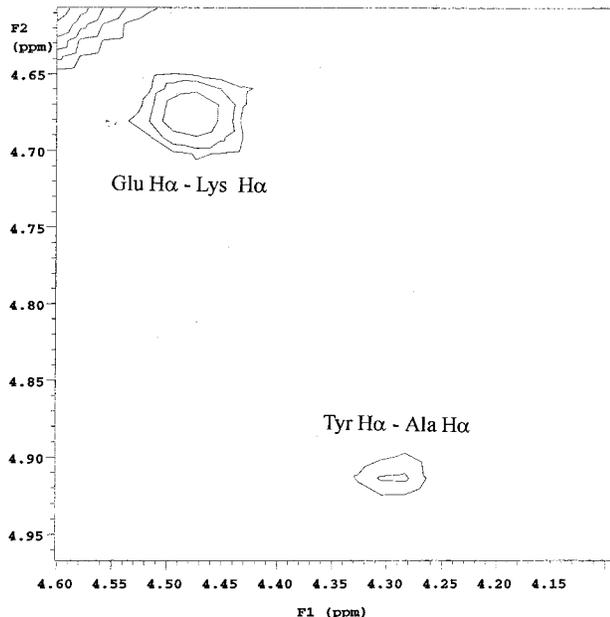

Figure 6. Selected ROESY data ($H_\alpha−H_\alpha$ NOEs) for YKA (conditions described in Figure 2).

than the $\Delta\delta_{H\alpha}$ values for AKL, which suggests a larger extent of β-hairpin folding for YKA than for AKL.

Additional Mutations: Focus on Diagonal Interactions. We tested the hypothesis that the diagonal Tyr-2/Lys-9 interaction stabilizes the β-hairpin conformation of YKL by expanding our studies to additional mutants. A favorable diagonal interaction between Tyr-2 and Lys-9 is not the only possible explanation for the greater β-hairpin stability manifested by YKA relative to AKL in the data presented above. At least three alternatives must be considered. (1) The β-hairpin conformation of parent peptide YKL might be stabilized by a favorable intrastrand side chain−side chain interaction between Tyr-2 and Glu-4, but not stabilized, or at least stabilized to a lesser extent, by an intrastrand interaction between Lys-9 and Leu-11. In this case, YKA would suffer less in terms of β-hairpin stability from the Leu → Ala mutation than would AKL from the Tyr → Ala mutation. This possibility arises because residues in *i* and *i*+2 positions of a β-strand are oriented on the same side of the
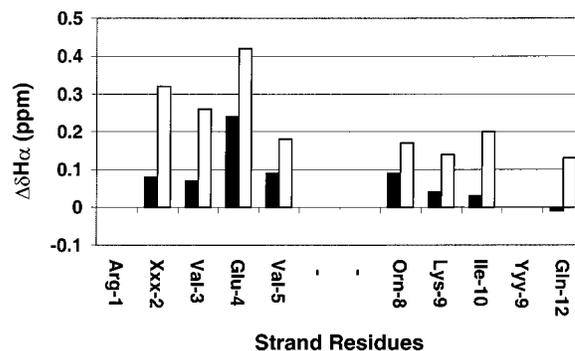

Figure 7. $\Delta\delta H\alpha$ (observed $\delta H\alpha$ − random coil $\delta H\alpha$) for AKL (solid bars, Xxx = Ala, Yyy = Leu) and YKA (open bars, Xxx = Tyr, Yyy = Ala). For both peptides, $\Delta\delta H\alpha$ of Yyy is zero. Random coil values were obtained from AKL-u and YKA-u, respectively. All peptides at 2 mM concentration in H_2O/D_2O (9:1 v/v; conditions as described in Figure 2).

Chart 1

strand; if the side chains of these residues were sufficiently large they might engage in a favorable interaction that stabilizes the extended backbone conformation and thereby contributes to overall β-sheet stability. (2) The β-hairpin conformation of parent peptide YKL might be destabilized by an unfavorable intrastrand side chain−side chain interaction between Lys-9 and Leu-11, but not destabilized, or at least destabilized to a lesser extent, by an intrastrand interaction between Tyr-2 and Glu-4. (3) The difference in β-hairpin conformational stability between YKA and AKL might result from a difference between the β-sheet propensities of Tyr and Leu. Indeed, Leu is commonly ranked below Tyr on β-sheet propensity scales.[55]

Alternative (1) seems unlikely because statistical surveys of the crystallographic database do not reveal significant $i \leftrightarrow i+2$ correlations in β-sheets of folded proteins.[31] In our peptides, a further argument against stabilizing interactions between Tyr-2 and Glu-4 (or between Lys-9 and Leu-11) arises from the lack of NOEs between these side chain pairs. Testing alternatives (2) and (3) provided motivation for the mutational studies described below.

Two pairs of mutant peptides, YKA/AKY and YSA/ASY (Chart 1), were examined in an effort to determine whether the interaction between diagonally juxtaposed side chains of NHB residues (e.g., Tyr-2 and Lys-9 in YKA) contributes to β-hairpin stability. Composition is identical within each pair, so differences in β-hairpin population within the pairs cannot arise from

(55) Muñoz, V.; Serrano, L. *Proteins: Struct. Funct. Genet.* **1994**, *20*, 301−311.

differences in the β-sheet propensities of individual residues. The first pair differs from the second in that Lys-9 is replaced with Ser. This mutation is expected to minimize diagonal interaction with Tyr-2 and minimize any intrastrand repulsion that might occur with Tyr-11, because the Ser side chain is considerably shorter than the Lys side chain. Ser is polar, which should promote aqueous solubility for YSA and ASY, despite the loss of the charged Lys side chain.

NOE data provided qualitative insight on the folding of YKA, AKY, YSA, and ASY. As noted above (Figure 5), YKA displays multiple interstrand NOEs that are consistent with the expected β-hairpin folding pattern. In contrast, isomer AKY shows only two interstrand NOEs, between NH of Val-5 and NH of Orn-8 and between $C_\alpha H$ of Glu-4 and $C_\alpha H$ of Lys-9. Thus, the NOE data provide evidence for formation of only the inner portion of the β-hairpin in AKY, which is comparable to the behavior of AKL (vide supra). YSA displays weak NOEs between $C_\alpha H$ of Tyr-2 and $C_\alpha H$ of Ala-11, and between $C_\delta H$ of Tyr-2 and $C_\beta H$ of Ala-11; no interstrand NOEs could be detected for inner portions of the expected β-hairpin conformation. No interstrand NOEs were observed for ASY, although resonance overlap would have prevented our detecting $C_\alpha H$- -$C_\alpha H$ NOEs for this peptide. Overall, the NOE data suggest that YKA forms a more stable β-hairpin than does AKY. Differences between YSA and ASY, if any, are more subtle. These qualitative conclusions support our hypothesis that interaction between the side chains of Tyr-2 and Lys-9 in YKL (and YKA) stabilizes the β-hairpin conformation.

Quantitative Analysis of β-Hairpin Formation. We sought to estimate the population of the β-hairpin conformations of YKA, AKY, YSA, and ASY to gain further insight on the relative stabilities of these folding patterns. $\delta_{H\alpha}$ data have previously been used to assess the extent of β-hairpin formation.[23,25,35,56] This type of measurement provides site-specific information at multiple independent positions along the backbone. Since short β-hairpins experience rapid conformational equilibration on the NMR time scale, one must estimate the $\delta_{H\alpha}$ values for the fully unfolded state and for the fully folded state to derive population information from $\delta_{H\alpha}$ values observed for an equilibrating β-hairpin.[10,11,25,57]

We have recently reported a new strategy for estimating $\delta_{H\alpha}$ values for the fully unfolded state (δ_U) and the fully folded state (δ_F) of equilibrating β-hairpins.[35] The unfolded state is represented by the D-Pro $\rightarrow$ L-Pro diastereomer (e.g., YKL-u is the unfolded reference for YKL). The folded state is represented by the cyclic peptide in which the termini of the linear peptide are connected by a second D-Pro-Gly loop segment, e.g., cyclo-(RYVEV^{D}PGOKILQ^{D}PG), designated YKL-f for the *f*olded
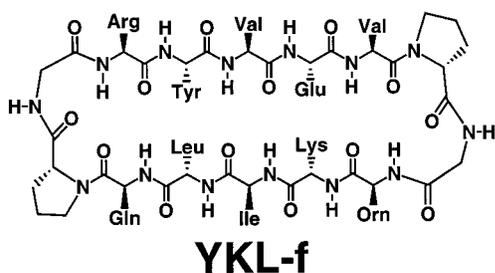
YKL-f

reference state. YKL-f displays numerous NOEs between nonadjacent residues, all of which are consistent with the

(56) For a clever alternative approach to quantitative analysis, see ref 28.

(57) Honda, S.; Kobayashi, N.; Munekata, E. *J. Mol. Biol.* **2000**, *295*, 269–278.
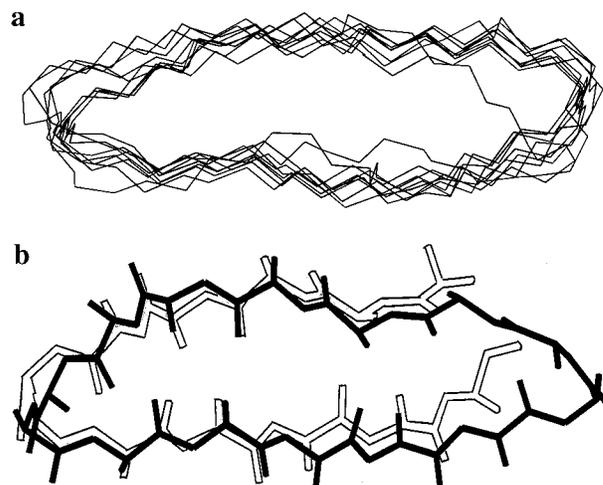

Figure 8. NOE-restrained dynamics results for YKL-f, using NOEs between protons on nonadjacent residues and NOEs between adjacent residues in the turn region. A total of 500 random structures were annealed by using the program DYANA with NOE restraints derived from NOESY and ROESY data. (A) Top view of the 10 best structures of YKL-f, backbone atoms only. (B) Overlay of the best structure of YKL (light) and the best structure of YKL-f (dark).

expected double-stranded β-sheet conformation. NOE-restrained dynamics was carried out with the program DYANA, but we were unable to generate a covalently closed backbone with this program. Therefore, the DYANA calculations were conducted with distance constraints intended to hold Arg-1 and Gly-14 in the proper juxtaposition (numbering as for linear peptides). The 10 lowest energy structures from this calculation were then minimized by using the SYBYL program (Tripos Software, St. Louis, MO) with a covalently closed backbone ring. (RMSD was not readily calculated after the SYBYL minimizations, but RMSD is 0.76 ± 0.26 Å for the 10 best structures, backbone atoms only, from the DYANA analysis, and no significant structural changes were observed after these minimizations.) Figure 8A shows the overlay of the 10 structures (backbone heavy atoms only) after SYBYL minimizations.

Several lines of evidence suggest that the cyclic peptide YKL-f is a good model for the fully folded state of YKL. Figure 8B shows an overlay of the best structures (backbone atoms) for YKL and YKL-f derived from NOE-restrained analysis (RMSD between these structures = 0.61 Å). Amide proton H/D exchange data (Figure 9) show that amide protons expected to form intramolecular hydrogen bonds display consistently larger protection factors than do amide protons expected to be exposed to solvent; some of the inward-facing amide protons exchange extremely slowly.[58] In addition, the $\delta_{H\alpha}$ values of YKL-f are unaffected by introduction of 30 vol % 2,2,2-trifluoroethanol (TFE; data not shown). Introduction of TFE or other alcohol cosolvents strongly enhances β-hairpin formation in linear peptides, as evidenced by increasing $\delta_{H\alpha}$ values.[23,25,26] The insensitivity of the $\delta_{H\alpha}$ values of YKL-f to added TFE strongly supports our conclusion that this cyclic peptide is fully folded in aqueous solution.

Although the $\delta_{H\alpha}$ approach provides data for each residue in YKL, only some sites along the backbone are suitable for monitoring the unfolded $\leftrightarrow$ β-hairpin equilibrium. The terminal residues (Arg-1 and Gln-12) are unsuitable because of high mobility. Strand residues in NHB positions, Tyr-2, Glu-4, Lys-9, and Leu-11, were found to be unsuitable as well (vide infra).

(58) Englander, S. W.; Kallenbach, N. R. *Quart. Rev. Biophys.* **1984**, *16*, 521–655.
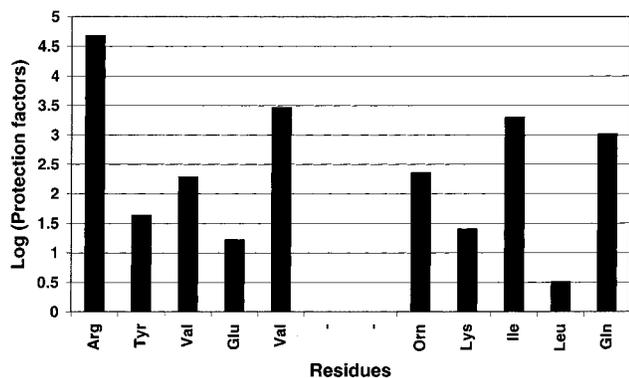
Figure 9. Log protection factors for H/D amide exchange of strand residues in YKL-f. The protection factor of a given residue is the rate constant for H/D amide exchange of that residue in YKL-f divided by the rate constant for amide H/D exchange of that residue in the random coil state; the latter values were estimated according to Bai and Englander (ref 66). H/D exchange studies were performed in D_2O, 100 mM sodium deuterioacetate buffer, pH 3.8 (uncorrected), 4 °C. One-dimensional ^1H NMR data were collected on a 500 MHz INOVA spectrometer. Amide NH groups that are expected to be solvent-exposed show log protection factors <2, while amide NH groups that are expected to be internally hydrogen bonded show log protection factors >2. Amide protons of Val-5 and Ile-10 showed negligible exchange over the course of the experiment (several months), which made it impossible to measure exchange rates reliably; the values shown for Val-5 and Ile-10 are derived from lower limits of the exchange rates for these residues.

Fortunately, strand residues in HB positions, Val-3, Val-5, Orn-8, and Ile-10, are suitable for monitoring β-hairpin population via $\delta_{H\alpha}$ data, as discussed below.

Figure 10 shows β-hairpin population for YKL at 4 °C in aqueous solution, as deduced from $\delta_{H\alpha}$ data at eight strand residues. In each case, the population was estimated by using eq 1, where δ_{obs} was obtained from YKL, δ_U was obtained from YKL-u, and δ_F was obtained from YKL-f. For the HB positions, Val-3, Val-5, Orn-8, and Ile-10, the deduced population varies

$$\beta\text{-hairpin population (\%)} = \frac{\delta_{obs} - \delta_U}{\delta_F - \delta_U} \qquad (1)$$

between 59% and 76% (Figure 10A; average = 68 ± 7%), which constitutes reasonably good internal agreement. As an independent check on the $\delta_{H\alpha}$-based population determination, we used the intensity of the $C_\alpha H$- -$C_\alpha H$ NOE between Tyr-2 and Leu-11 of YKL to estimate β-hairpin population under identical conditions. This estimate was obtained by assuming that the observed NOE intensity arises entirely from the β-hairpin conformation and that the $C_\alpha H$- -$C_\alpha H$ separation in this folded conformation is 2.32 Å (ref 50). It should be noted that the use of NOE data for estimating folded populations in flexible peptides is inherently imprecise because the NOE intensity depends on the reciprocal of the distance between the protons in question to the sixth power,[50] and small errors in assumed H- -H separation in the folded state lead to large errors in deduced population. Nevertheless, the NOE-based β-hairpin population estimate, ca. 50%, displays reasonable agreement with the $\delta_{H\alpha}$-based population determination.[59]

---

(59) We were unable to use the $C_\alpha H$- -$C_\alpha H$ NOE between Glu-4 and Lys-9 of YKL to estimate β-hairpin population because the $C_\alpha H$ resonances were too close to the residual water resonance; a similar problem prevented use of the $C_\alpha H$- -$C_\alpha H$ NOE between Tyr-2 and Leu-11 of YKL-f as a reference for population calculation with the $C_\alpha H$- -$C_\alpha H$ NOE between Tyr-2 and Leu-11 of YKL.
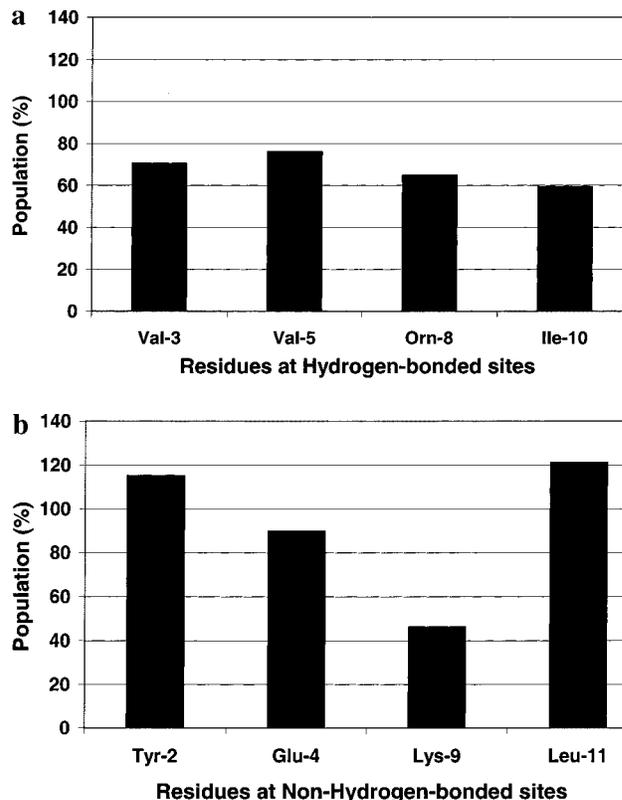

Figure 10. $\delta H\alpha$ value-based β-hairpin population calculated at each strand residue at 4 °C. (A) Strand residues at hydrogen bonded sites. (B) Strand residues at non-hydrogen bonded sites. The population at hydrogen bonded sites has an average value of 68 ± 7%, while the population at non-hydrogen-bonded sites shows more variation (93 ± 34%). Hα resonances of peptides YKL-f and YKL-u were used as references for the fully folded and unfolded states, respectively. The population at Arg-1 is not shown because the N-terminus is uncapped; the population at Gln-12 is not shown because of end-fraying effects. (Conditions as described in Figure 2.)

In contrast to the consistency among the population estimates at the HB strand residues of YKL (Figure 10A), there is considerable variation among YKL population estimates derived from $\delta_{H\alpha}$ data for the NHB strand residues, Tyr-2, Glu-4, Lys-9, and Leu-11 (Figure 10B). The deduced β-hairpin populations range from 45% to 120% for the NHB residues. We conclude from the apparently nonsystematic variation that the NHB residues are unsuitable for population analysis in YKL. Why does the $\delta_{H\alpha}$ approach fail for the NHB residues? We suspect that there are subtle differences in interstrand side chain packing between cyclic peptide YKL-f and the folded state of YKL. Particularly critical in this regard is the aromatic side chain of Tyr-2. Variations in average Tyr side chain orientation sufficient to cause only 0.2 ppm differences between NHB $\delta_{H\alpha}$ values in the folded state of YKL vs YKL-f would account for the "scatter" observed among the population values deduced for the NHB residues (Figure 10B). We have recently observed a similar distinction between HB and NHB residues in population analysis of a completely different designed β-hairpin:[40] the NHB residues gave widely scattered population estimates, but the HB residues provided population estimates that were consistent with one another and with an independent NOE-based population estimate. Therefore, we conclude that cyclic peptides such as YKL-f represent useful references for the $\delta_{H\alpha}$ data of HB residues in the folded state of linear β-hairpin-forming peptides such as YKL, despite the possibility of variations between side
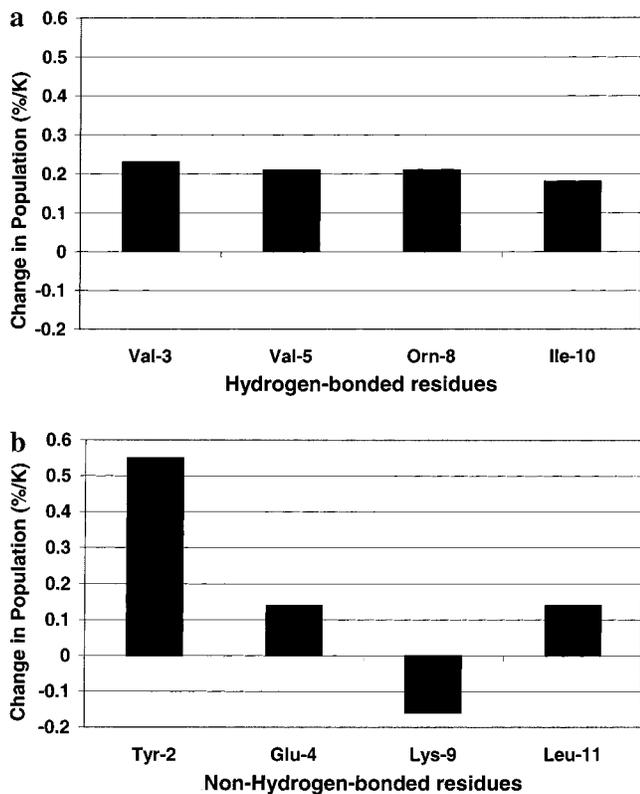
8674   *J. Am. Chem. Soc., Vol. 123, No. 36, 2001*

Syud et al.

Figure 11. Temperature-induced changes in hairpin population at internal strand residues for 2 mM YKL in H_2O/D_2O (9:1 v/v; conditions as describe in Figure 2). (A) Strand residues at hydrogen bonded sites. (B) Strand residues at non-hydrogen bonded sites. The change in population at hydrogen-bonded sites has an average value of 0.21 ± 0.02%/°C, while the change in population at non-hydrogen-bonded sites shows more variation (0.17 ± 0.29%/°C). The deduced population at every residue changed linearly over a temperature range of 4−75 °C.

chain packing in the cyclic peptide and in the fully folded state of the linear peptide.

Variable-temperature studies offer further evidence that $\delta_{H\alpha}$ data for the HB strand residues of YKL, YKL-u, and YKL-f provide consistent and therefore reliable insight on β-hairpin population, while $\delta_{H\alpha}$ data for the NHB strand residues are inconsistent and therefore unreliable. Figure 11A shows the change in percent of β-hairpin population between 4 and 75 °C deduced for the HB residues, and Figure 11B shows the population changes deduced for the NHB residues. The HB residues display very consistent temperature-induced effects, with an average β-hairpin population decrease of 0.21 ± 0.02%/°C (i.e., from an average of 68% at 4 °C to an average of 53% at 75 °C). In contrast, the NHB residues display markedly inconsistent effects, with the data for one residue (Lys-9) implying that the β-hairpin becomes more stable at elevated temperature. This difference between HB and NHB residues matches behavior we have observed for a different designed β-hairpin;[40] the similarities between the two systems reinforce our general conclusion that $\delta_{H\alpha}$ data for HB residues (but not NHB residues) provide a reliable indication of β-hairpin population. The consistency of the thermally induced population changes at four independent strand positions of YKL (Figure 11A) suggests that β-hairpin formation in this peptide is cooperative, i.e., that the folded state forms and unravels in a coordinated manner.

Since we are confident that interpolation of $\delta_{H\alpha}$ values for HB residues of YKL between reference values obtained for YKL-u and YKL-f provides a reliable assessment of β-hairpin

Table 1. Population of the β-Hairpin State for Linear Peptides[a]

model	Val-3	Orn-8	Ile-10	average
I	70	65	59	65 ± 6%
II	47	67	65	60 ± 11%
III	37	56	53	49 ± 10%
IV	45	60	59	55 ± 8%
V	72	97	100	90 ± 15%

[a] The population of the β-hairpin state for each linear peptide was calculated at each indicator residue from $\delta_{H\alpha}$ data as $(\delta_{obs} - \delta_U)/(\delta_F - \delta_U) \times 100$. The five models differ in the source of the δ_U and δ_F values, as discussed in the text.

population, we can use NMR data for YKL to evaluate alternative approaches to β-hairpin population analysis. A number of general δ_U data sets have been reported, some measured with short peptides that cannot adopt a stable fold in solution (e.g., Gly-Gly-Xxx-Ala (ref 50) or Ac-Gly-Gly-Xxx-Ala-Gly-Gly-NH$_2$ (ref 54b)) and others extracted statistically from unordered segments of protein structures determined by NMR (e.g., ref 53a). The latter approach can also be used to create a general δ_F data set, based on β-sheets in protein structures determined by NMR. Alternatively, some workers have tried to identify δ_F values for specific peptides by using solvent additives (typically methanol (MeOH) or 2,2,2-trifluoroethanol (TFE)) to enhance β-hairpin population, relative to pure water. In this approach, β-hairpin population is monitored (often by CD) as cosolvent is titrated into an aqueous solution of the peptide. Initially, cosolvent addition leads to increased β-hairpin population, but at some point during the titration, often around 40−50 vol % MeOH or TFE, the cosolvent effect disappears: adding further alcohol does not lead to further increase in β-hairpin population. This "plateau" state is then assumed to represent 100% β-hairpin.

Each of these strategies for identifying δ_U or δ_F values has potential problems with regard to β-hairpin population determination. Use of short nonfolding peptides or a structure database will provide chemical shift values that do not reflect the local sequence context of individual residues in a specific peptide like YKL. However, if we focus on HB strand residues in a β-hairpin (i.e., residues for which the C_α−H bond is oriented away from the other strand), perhaps these local sequence effects will be minimized. Use of a cosolvent-stabilized state for δ_F values is problematic because the cosolvent may exert an intrinsic effect on $\delta_{H\alpha}$ values, relative to aqueous solution. An even bigger potential problem is that the "plateau" state may not represent 100% β-hairpin population. TFE titrations of α-helix forming peptides typically lead to a plateau around 40 mol % TFE, but results from Luo and Baldwin[60] indicate that this plateau does *not* necessarily represent 100% α-helix population.

Table 1 compares β-hairpin estimates for YKL obtained by using different δ_U and δ_F values. Results from Wishart et al. imply that δ_F values obtained via statistical analysis of β-sheets in proteins should not be applied to residues preceding proline;[54b] therefore, we have used only three HB residues of YKL, Val-3, Orn-8, and Ile-10, for our analysis. For the ornithine residue we use lysine values from the literature. Results of five analyses are summarized in Table 1. Model I is analysis using δ_U and δ_F values YKL-u and YKL-f. In models II−IV the δ_F values are derived from statistical analysis of β-sheets in protein NMR structures.[53a] In model II, δ_U values are derived from statistical analysis of unordered regions in protein NMR structures.[53a] In model III, δ_U values are obtained from Gly-Gly-Xxx-Ala peptides.[50] In model IV, δ_U values are obtained from Ac-Gly-

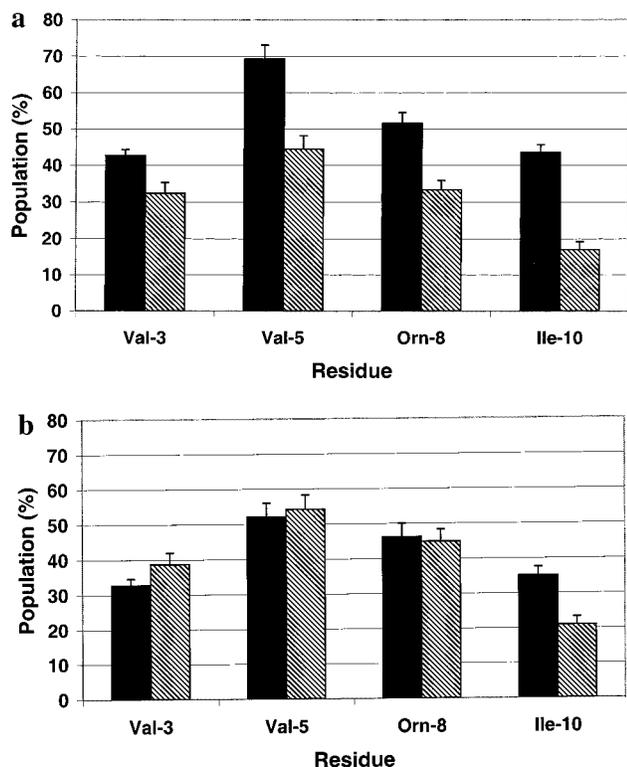(60) Luo, P.; Baldwin, R. L. *Biochemistry* **1997**, *36*, 8413−8412.

Figure 12. (A) δHα value-based β-hairpin population at 4 °C of YKA (solid bars) and AKY (striped bars) calculated at each hydrogen bonded strand residue. (B) δHα value-based β-hairpin population at 4 °C of YSA (solid bars) and ASY (striped bars) calculated at each hydrogen bonded strand residue. Conditions as described in Figure 2.

Gly-Xxx-Ala-Gly-Gly-NH$_2$ peptides.[54b] In model V, δ_F values are obtained from YKL in 40 vol % TFE (we confirmed that β-hairpin population maximizes at this solvent composition), and δ_U values are derived from statistical analysis of unordered regions in protein NMR structures.[53a]

The population averages for YKL derived from models II–IV are comparable to those obtained by using YKL-u and YKL-f as reference peptides. However, when we used models II–IV for analysis of YKA, AKY, YSA, and ASY the results were significantly poorer (greater uncertainty) than those obtained by using the appropriate L-Pro and cyclic reference peptides (model I). For example, analysis of AKY with reference peptides (model I) indicated 27 ± 9% β-hairpin population, based on data for Val-3, Orn-8, and Ile-10, while analysis with models II–IV gave 23 + 22%, 10 ± 20%, and 14 ± 18% β-hairpin, respectively.

The results for YKL analysis with model V (Table 1) show that this approach leads to an over-estimation of β-hairpin population. This result is in line with the conclusion of Luo and Baldwin[60] that limiting states obtained during solvent titrations do not necessarily represent 100% folding for α-helical peptides. We conclude that cosolvent-induced folded states cannot be relied upon as references for 100% β-hairpin formation.

Quantitative Comparison of Mutant Peptides. The results in the preceding section suggest that we may use β-hairpin population estimates derived from $\delta_{H\alpha}$ data for the four internal HB strand positions to monitor how mutations at NHB strand positions affect β-hairpin stability. Figure 12 shows β-hairpin populations at 4 °C calculated for YKA, AKY, YSA, and ASY at each of the four internal HB strand residues. The population values have been calculated with eq 1, i.e., for each mutant we have used the L-Pro diastereomer (YKA-u, AKY-u, YSA-u, or

AYS-u) to estimate δ_U and the cyclic analogue (YKA-f, AKY-f, YSA-f, or AYS-f) to estimate δ_F. At each residue the deduced β-hairpin population for YKA is greater than that for AKY (Figure 12A), which is consistent with our NOE-based conclusions (vide supra). In contrast, the deduced β-hairpin populations for YSA and ASY are comparable (Figure 12B).

The greater population of the β-hairpin formed by YKA relative to the β-hairpin formed by isomer AKY suggests that diagonal side chain–side chain interactions between Tyr-2 and Lys-9 in YKA contribute to β-hairpin stability. This conclusion is supported by the similar stabilities of the β-hairpins formed by isomers YSA and ASY, since the Ser side chain should be too short to engage in a favorable interaction with Tyr-2 in YSA. Comparisons involving YKA, AKY, YSA, and ASY make it unlikely that the β-hairpin stabilization conferred by Tyr in position 2 relative to Tyr in position 11 stems from loss of an intrastrand side chain–side chain repulsion between Tyr-11 and either Lys-9 or Ser-9. For the peptides with Tyr-2, an analogous intrastrand repulsion would be possible with Glu-4. Although one might argue that Lys-9 is more susceptible to such repulsions because the side chain is larger than that for Glu-4, this argument could not be extended to Ser-9, the side chain of which is smaller than that of Glu-4.

Table 2 presents the populations deduced at the four internal HB residues for peptides YKL, YKA, AKY, YSA, and ASY, and summarizes the lateral and diagonal pairings for residues 2, 9, and 11 in these peptides. Side chain pairings that are expected to contribute little or nothing to β-hairpin stability are shown in parentheses. This data summary, suggested by a reviewer, helps one see why we conclude that both the lateral Tyr-2/Leu-9 interaction and the diagonal Tyr-2/Lys-9 interaction contribute to the stability of the β-hairpin formed by YKL.

Discussion

Evaluation of sequence-stability relationships among autonomously folding helical peptides at both qualitative and quantitative levels has provided numerous important insights on the factors that influence this common secondary structure.[7,8] Several laboratories, including ours, have been motivated to identify autonomously folding β-hairpin peptides so that comparable advances can be achieved in our understanding of antiparallel β-sheet secondary structure.[10,11] β-Hairpin model systems have been used to show that interstrand interactions between side chains of NHB residues confer stability on the antiparallel β-sheet,[23–28] and our results provide further evidence for this general conclusion. More importantly, however, our data suggest that diagonal side chain–side chain interactions are energetically significant; we estimate that this interaction contributes on the order of 0.5 kcal/mol to the stability of the β-hairpin conformation of YKL.

We have tested the diagonal interaction hypothesis via comparisons within two isomeric peptide pairs, YKA vs AKY and YSA vs ASY. When residue 9 is Lys, β-hairpin stability is higher when the Tyr residue is near the N-terminus (YKA) than when the Tyr is near the C-terminus (AKY). The lack of a significant stability difference between the β-hairpins formed by YSA and ASY shows that Lys at residue 9 is essential for manifestation of the Tyr positional effect. Only the N-terminal position of Tyr allows an intramolecular diagonal contact with Lys-9 in a β-hairpin with a right-handed twist; therefore, our observations suggest that favorable contacts between the side chains of Tyr-2 and Lys-9 (in YKA) contribute to overall stability of the β-hairpin conformation of these peptides. The population differences between YKA and AKY (Figure 12) are

Table 2. Population of the β-Hairpin State for Linear Peptides[a]

peptide	lateral pairing[b]	diagonal pairing[b]	Val-3	Val-5	Orn-8	Ile-10
YKL	Tyr-2/Leu-11	Tyr-2/Lys-9	70 ± 2%	76 ± 4%	65 ± 3%	59 ± 2%
YKA	(Tyr-2/Ala-11)	Tyr-2/Lys-9	43 ± 2%	69 ± 4%	52 ± 3%	43 ± 2%
AKY	(Ala-2/Tyr-11)	(Ala-2/Lys-9)	32 ± 3%	44 ± 4%	33 ± 3%	17 ± 2%
YSA	(Tyr-2/Ala-11)	(Tyr-2/Ser-9)	33 ± 2%	52 ± 4%	46 ± 4%	35 ± 3%
ASY	(Ala-2/Tyr-11)	(Ala-2/Ser-9)	39 ± 3%	54 ± 4%	45 ± 3%	21 ± 2%

[a] The population of the β-hairpin state for each linear peptide was calculated at each indicator residue from $\delta_{H\alpha}$ data as $(\delta_{obs} - \delta_U)/(\delta_F - \delta_U) \times 100$. Experimental uncertainties reflect the ±0.01 ppm uncertainty in the $\delta_{H\alpha}$ measurements. [b] Pairings in parentheses are not expected to contribute significantly to β-hairpin stability, because at least one of the side chains is too short.

comparable to differences in helix population associated with *i*, *i*+4 relative to *i*, *i*+3 spacing of large side chains.[61] This similarity suggests that the energetic contributions of diagonal side chain interactions to β-hairpin stability are comparable to the energetic contributions of *i*, *i*+4 side chain interactions to helix stability. We are aware of only one prior discussion of diagonal interactions within antiparallel β-sheet, in a recent statistical survey of the protein structure database.[48] Other surveys have focused by design on lateral interstrand pairings.[31,32] Cootes et al.[48] undertook what they described as a "physically naive" analysis of pairwise residue interactions within regular secondary structures, an analysis in which they did not specify any particular juxtaposition between the residues, but instead tried to consider all possible juxtapositions. Many of the interaction patterns they identified were expected, e.g., lateral HB and NHB interstrand pairings in the antiparallel β-sheet. These workers were surprised, however, to find a correlation in antiparallel β-sheets that corresponds to what we call a diagonal interaction ("*i* → *j*−2" in their terminology). Cootes et al.[48] noted that this pairing is directional in the manner expected given the right-handed twist preference of strands in β-sheets. Our diagonal interaction hypothesis is consistent with the analysis of Cootes et al.

Conclusions

Our findings provide further support for the general view that side chain−side chain interactions are critical determinants of antiparallel β-sheet stability. Thus, even though the D-Pro-Gly loop segment is a strong promoter of β-hairpin folding, the favorability of this loop segment cannot alone account for the high population of the β-hairpin conformation displayed by 12-residue peptide YKL in aqueous solution. Consistent with the results of statistical surveys of protein crystal structures and previous analysis of designed β-hairpin peptides, our data suggest that interactions between hydrophobic side chains that are laterally paired in NHB positions on adjacent strands contribute to antiparallel β-sheet stability. In addition, our data provide evidence that diagonal side chain−side chain interactions can stabilize an antiparallel β-sheet.

This study should focus attention on diagonal side chain−side chain interactions in the antiparallel β-sheets of proteins. The diagonal interaction was not envisioned in the original design of YKL, and it is possible that other diagonal residue pairings and/or other β-sheet contexts could lead to larger effects on stability than we observe. Analysis of diagonal interactions in other secondary and tertiary structural model systems should reveal the overall significance of this interaction in proteins.

Materials and Methods

Peptide Synthesis. Linear peptides were prepared with SYNERGY automated synthesizers (Applied Biosystems). Standard solid-phase Fmoc chemistry with HBTU activation and Rink Amide AM resin

(Applied Biosystems) were used at a 25 μmol scale. This resin produces peptides with a primary amide group at the C-termini; N-termini were not capped. Peptides were cleaved from the resin and side chains deprotected simultaneously using trifluroacetic acid (TFA). Peptides were purified by HPLC with a C4-silica column (5 μm, 10 × 250 mm; Vydac) and CH₃CN/H₂O/TFA eluents. Homogeneity was established by analytical HPLC with a C4-silica analytical column (5 μm, 4 × 250 mm; Vydac) and CH₃CN/H₂O/TFA eluents. Peptide identity was confirmed initially by matrix-assisted laser desorption time-of-flight mass spectroscopy, and subsequently by high-resolution ¹H NMR analysis.

Cyclic peptides were synthesized using an orthogonally protected glutamic acid derivative and standard solid-phase synthesis.[62] *N*-Fmoc-Glutamic acid α-allyl ester (Novabiochem) was coupled to Rink Amide AM resin (Applied Biosystems) through the unprotected side chain. The rest of the peptide was synthesized on resin using solid-phase methods as described above, but the final Fmoc group was not removed. The α-allyl group was removed with Pd(PPh₃)₄ in CHCl₃:AcOH:4-methylmorpholine (37:2:1). After removal of the N-terminal Fmoc group with piperidine, cyclization was achieved using HATU. Cyclic peptides were cleaved from the resin and the side chains deprotected with TFA; this process converted the glutamic acid to a glutamine residue. Cyclic peptides were isolated as described above.

Nuclear Magnetic Resonance. NMR samples were prepared by dissolving lyophilized peptides in H₂O/D₂O (9:1 ratio) or pure D₂O, 100 mM sodium deuterioacetate buffer, with pH adjusted to 3.8 with NaOH or NaOD (pH measurements were not corrected for isotope effects). Peptide concentrations were generally 1−2 mM. 2,2-Dimethyl-2-silapentane-5-sulfonate (DSS; Merck) was added to samples as internal reference.

NMR experiments were performed on a Varian INOVA 500 MHz spectrometer at 277 K; additional ROESY data were obtained for YKL and YKL-f using a Bruker AVANCE 750 MHz spectrometer. All two-dimensional spectra were acquired in the phase-sensitive mode with hypercomplex phase cycling (States-Haberkorn method). Solvent suppression was achieved by 0.6−0.7 ms presaturation during relaxation. A spectral window of 5500 Hz was used. Standard Varian pulse sequences were used, and data were processed using Varian VNMR version 5.3 software. Sine or cosine squared window functions were generally applied after baseline correction. For chemical shift and structure assignment COSY,[63] TOCSY,[64] NOESY,[65] and ROESY[64,66] experiments were performed by collecting 2048 points in f2 and 400−600 points in f1. TOCSY experiments employed a standard MLEV-17 spin lock sequence with a spin lock field of 7−8 kHz and mixing time of 80 ms, and for ROESY experiments 3 kHz and 200 ms, respectively. NOESY spectra utilized a mixing time of 100−200 ms. ROESY and NOESY spectra were compared to ensure the absence of spin diffusion. The ¹H chemical shift assignment of the peptide was achieved by the sequential assignment procedure.[50]

H/D amide exchange studies[67] were performed by dissolving lyophilized peptide in D₂O, 100 mM sodium deuterioacetate buffer,

(61) Padmanabhan, S.; Baldwin, R. L. *J. Mol. Biol.* **1994**, *241*, 706−713. Padmanabhan, S.; Baldwin, R. L. *Protein Sci.* **1994**, *3*, 1992−1997.

(62) Kates, S. A.; Sole, N. A.; Johnson, C. R.; Hudson, D.; Barany, G.; Albericio, F. *Tetrahedron Lett.* **1993**, *34*, 1549−1552.

(63) Aue, W. P.; Bartholdi, E.; Ernst, R. R. *J. Chem. Phys.* **1976**, *64*, 2229−2246.

(64) Bax, A.; Davis, D. G. *J. Magn. Reson.* **1985**, *65*, 355−360.

(65) Jeener, J.; Meier, B. H.; Bachmann, P.; Ernst, R. R. *J. Phys. Chem.* **1979**, *71*, 4546−4553.

(66) Bothner-by, A. A.; Stephens, R. L.; Lee, J. M.; Warren, C. D.; Jeanloz, R. W. *J. Am. Chem. Soc.* **1984**, *106*, 811−813.

with pH adjusted to 3.8 with NaOD (pH measurements were uncorrected for isotope effects) at 4 °C. One-dimensional ^{1}H NMR measurements were made every 5 min for 5 h, every 60 min for the subsequent 24 h, and, if necessary, on subsequent days over the next several weeks. The NMR sample was maintained at 4 °C. Data were collected on a 500 MHz INOVA spectrometer with 8 scans for the first 5 h and 100 scans thereafter in 20 800 data points. No water presaturation was applied. The spectra were analyzed using Varian VNMR version 5.3 software. The amide resonances were integrated and normalized to the well-resolved aromatic proton resonances of the tyrosine residue in the peptide. The rate constants for the decay of the resonances over time were calculated by least-squares fitting to single exponentials using the Igor Pro program (Wavemetrics, Inc.).

NOE-Restrained Dynamics. Simulations were performed for YLK and YKL-f using the program DYANA.[51] NOE restraints were derived from NOESY and ROESY data. Only long-range (between nonadjacent residues) and turn-defining NOEs were used for dynamics analysis. NOE intensities were qualitatively assigned to be strong, medium, weak, or very weak, and assigned constraints of 3, 4, 5, and 6 Å, respectively; a total of 36 restraints were used for YKL-f and 30 for YKL. DYANA was used to generate 500 random structures of YKL, which were subsequently annealed. The RMS deviation among the 10 best structures (fewest restraint violations) for YKL was 1.02 ± 0.34 Å (backbone atoms only). Analysis of YKL-f required a more complicated protocol because of the backbone cyclization. YKL-f was generated in DYANA by cyclizing the linear 14-residue peptide with distance constraints in place of a C−N bond between Arg-1 and Gly-14 (numbering follows linear peptides). Specifically, upper distance limits were used between three atoms pairs, Arg-1 N and Gly-14 N (3.0 Å), Arg-1 Hβ (pseudoatom) and Gly-14 N (6.0 Å), and Arg-1 N and Gly-14 carbonyl C (1.3 Å; this restraint was both an upper and a lower limit). The 10 best structures for YKL-f were then energy minimized using the program SYBYL (Tripos Software, St. Louis, MO) in 100 iterations using steepest descent. These minimizations ensured proper cyclization of the backbone through Arg-1 and Gly-14. RMS deviation among the 10 best YKL-f structures (out of 500) from DYANA was 0.76 ± 0.26 Å (backbone atoms only), but the analogous value was not available from the SYBYL analysis. However, there was very little structural change after the SYBYL minimizations. For both YKL and YKL-f the NOE-restrained computational analysis suggested a single family of folded conformations.

Aggregation Studies. Analytical ultracentrifugation (Beckman) experiments were carried out at 4 °C on the following peptide sets (L-Pro, D-Pro, and cyclic peptides where appropriate): octamer, YKL, AKL, YKA, and AKY. The peptides were studied at their respective NMR sample concentrations and at lower concentrations in H$_2$O/D$_2$O (9:1 ratio), 100 mM sodium deuterioacetate buffer, with pH adjusted to 3.8 with NaOH (pH measurements were not corrected for isotope effects). Revolution speeds of 44 and 56 K/min were used. Data were analyzed using the Igor Pro program (Wavemetrics, Inc.). Peptides were found to be monomeric in all cases. Figure 13 shows data obtained with 2 mM YKL under conditions used for NMR studies.

(67) Bai, Y.; Milne, J. S.; Mayne, L.; Englander, S. W. *Proteins: Struct. Funct. Genet.* **1993**, *17*, 75−86.
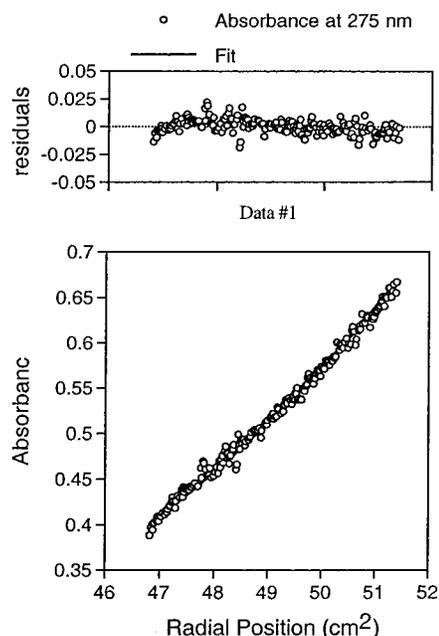

Figure 13. Sedimentation equilibrium analysis of YKL carried out under conditions used for NMR studies (Figure 2). The solid line was generated by fitting the data to behavior of a single ideal species. A molecular weight of 1260 was deduced; the theoretical molecular weight of YKL is 1416. The deviation may reflect nonideality that results from electrostatic repulsions between peptide molecules, which have a net charge ≥ +3.

CD and NMR were also used to study the aggregation of all peptides described here. High-resolution one-dimensional ^{1}H NMR of all the peptides showed sharp amide resonances, with doublets resolved at the baseline. There was no concentration dependence of either the CD signal or NMR ^{1}H chemical shifts between 1 and 0.05 mM.